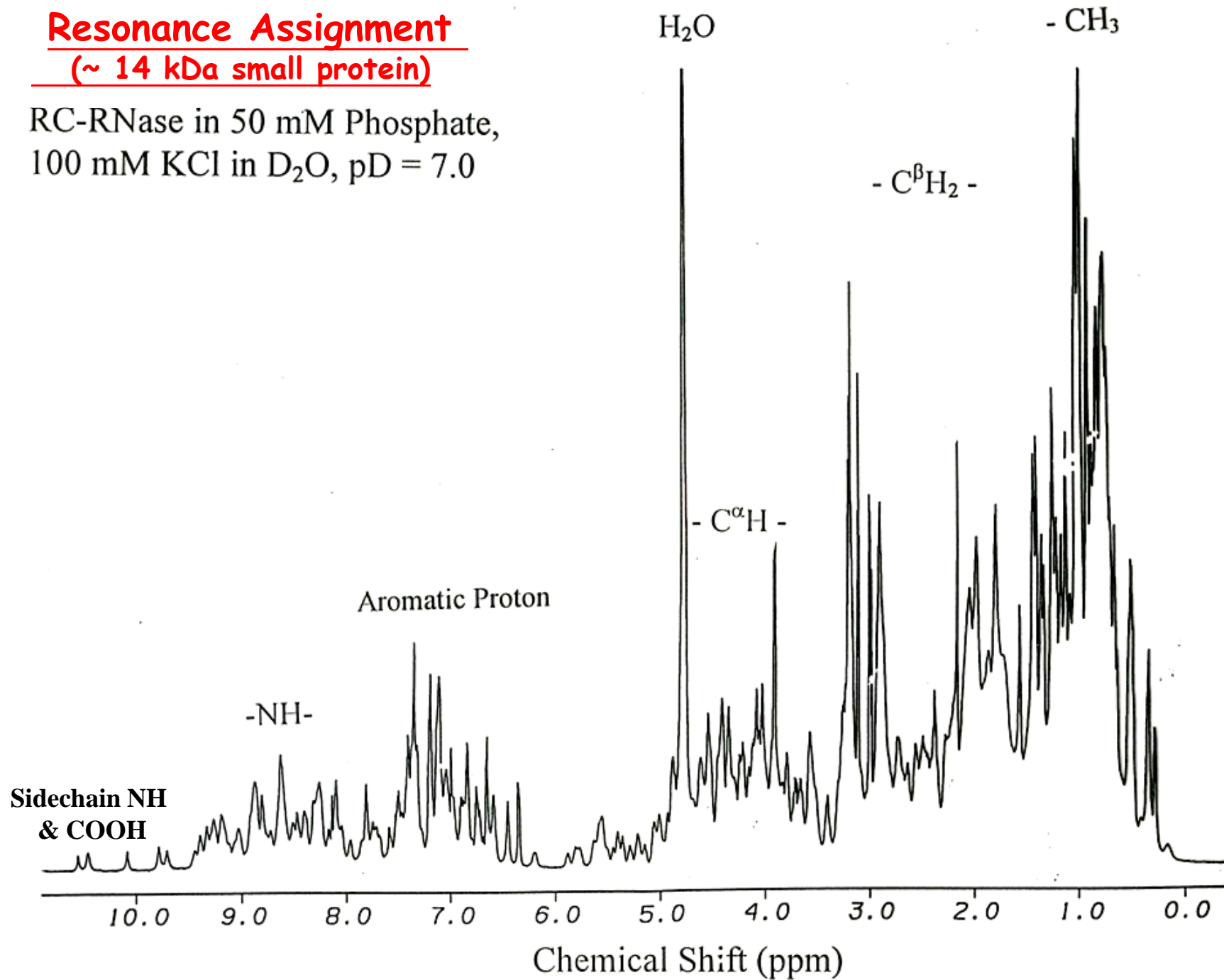


<u>Lect #</u>	<u>Date</u>	<u>Topics</u>
1	9/21	NMR and Energy level
2	10/5	1. Introduction to NMR spectroscopy
3	10/8	2. Practical aspects of acquiring NMR spectra
4	10/12	3. Introduction to signal processing
5	10/15	4. Quantum mechanical description of NMR
6	10/22	5. Quantum mechanical description of a one pulse experiment
7	10/26	6. The density matrix and product operators
8	10/29	Cancelled
9	11/2	7. Scalar coupling
10	11/5	Cancelled
11	11/9	8. Coupled spins: Density matrix and product operator formalism
12	11/12	Cancelled
13	11/16	9. Two-dimensional homonuclear J-coupled spectroscopy
14	11/19	Cancelled
15	11/30	10. Two-dimensional heteronuclear J-correlated spectroscopy
16	12/7	11. Coherence editing: Pulse-field gradients and phase cycling
17	1/4/2011	Review
18	1/11/2011	Final exam
		12. Quadrature detection in multi-dimensional NMR spectroscopy
		14. Resonance Assignments: Heteronuclear methods Selective topics

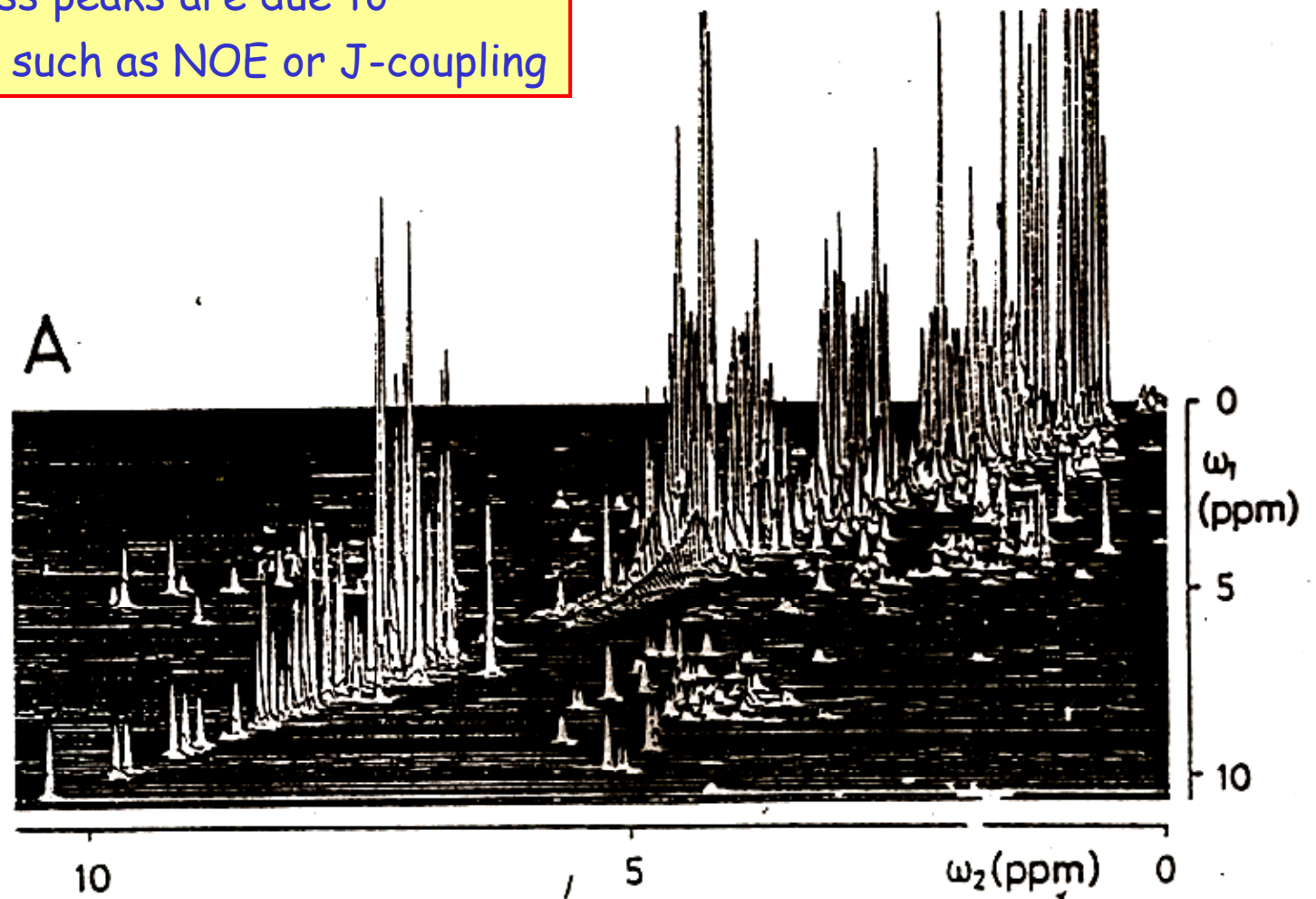
Resonance Assignment (~ 14 kDa small protein)

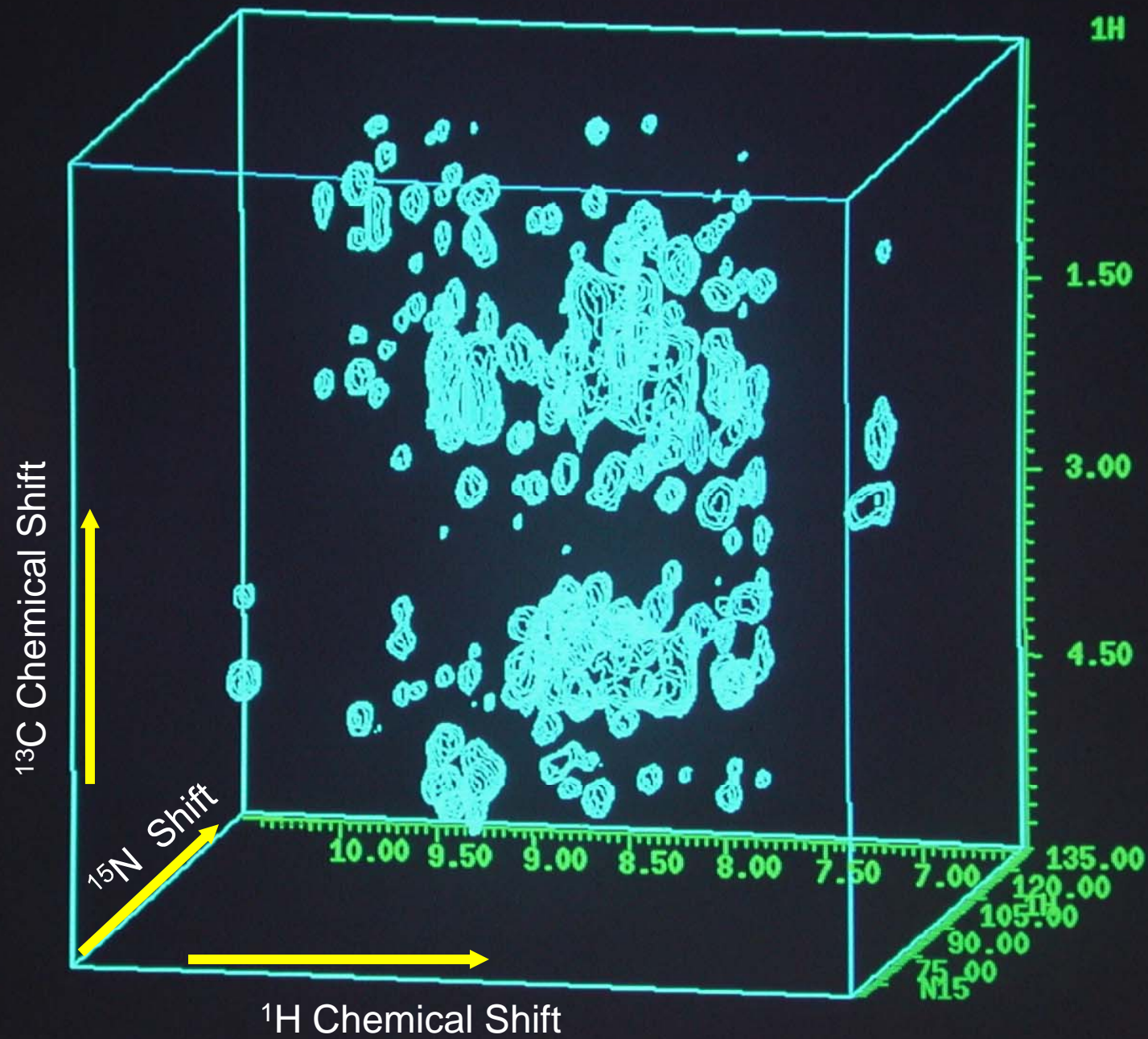
RC-RNase in 50 mM Phosphate,
100 mM KCl in D₂O, pD = 7.0



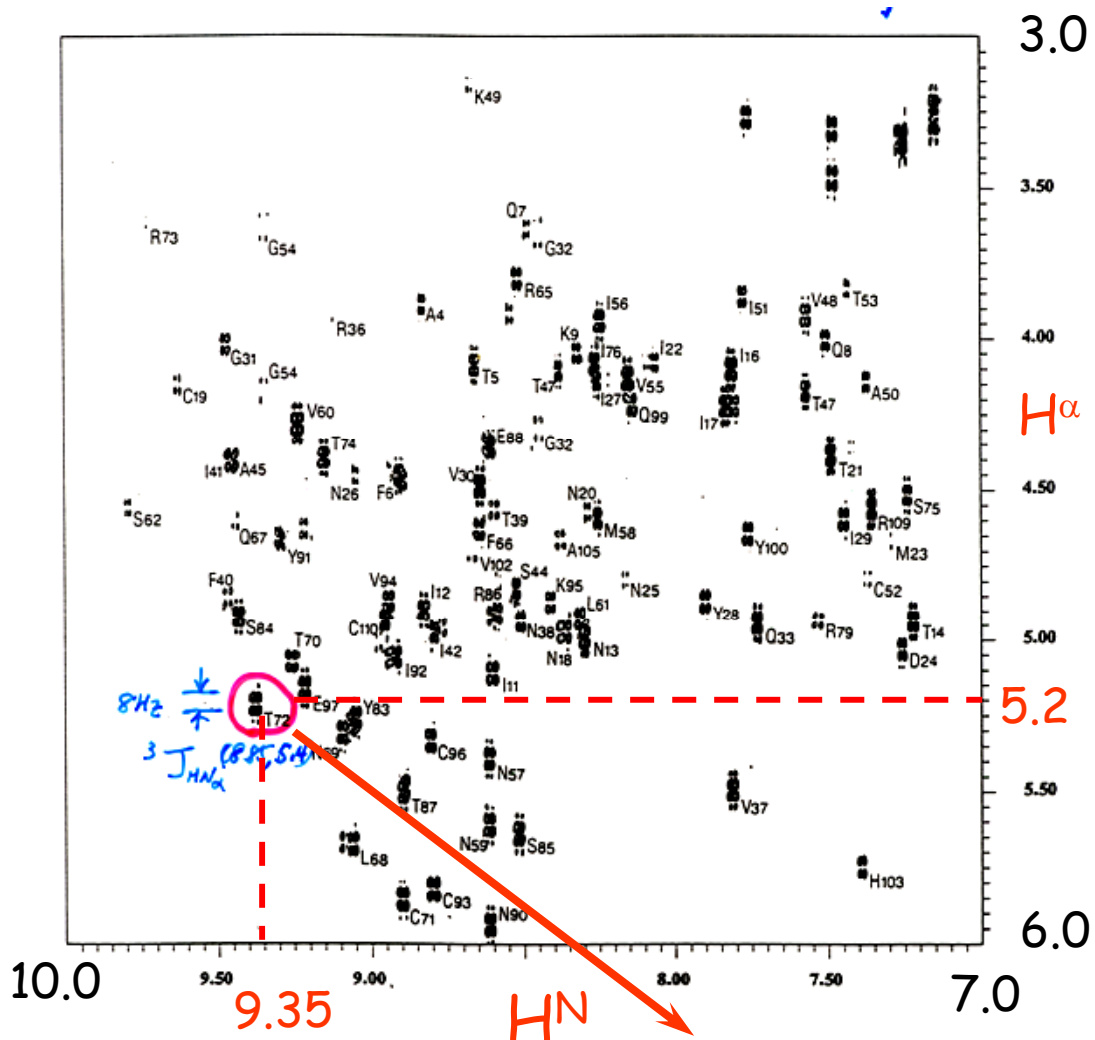
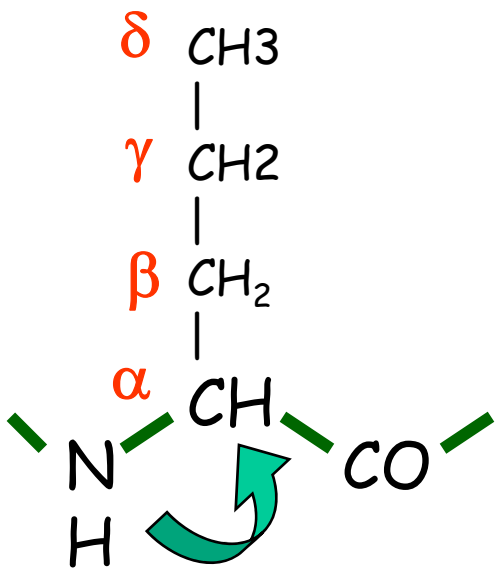
2D-NMR Spectrum

- Diagonal resonances same as in 1D spectrum
- off-diagonal cross peaks are due to **interactions** such as NOE or J-coupling

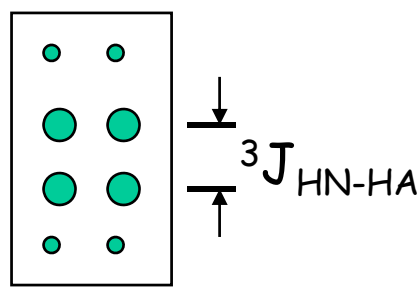




DQF-COSY (Fingerprint region)

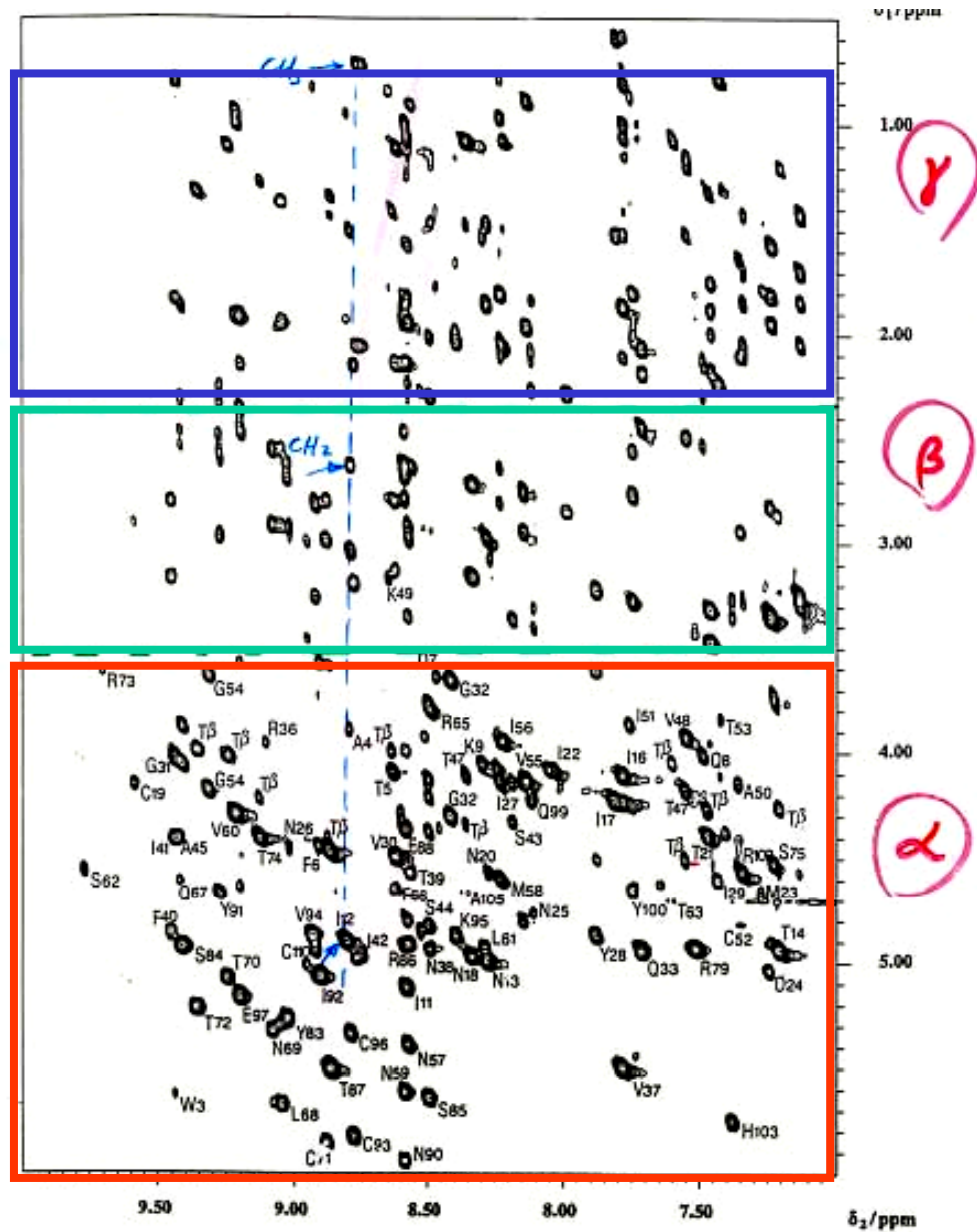
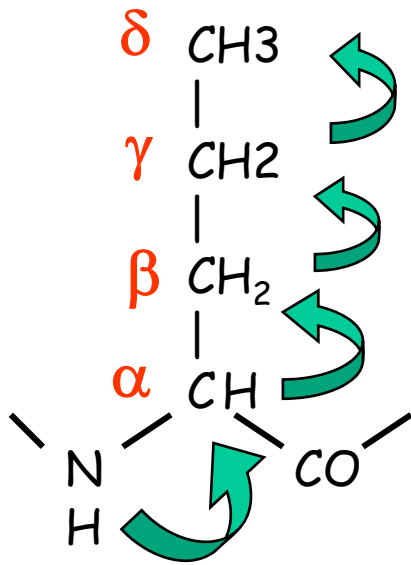


1. See only H^N and H^α correlation
2. $H^N - H^\alpha$ coupling can be measured



TOCSY (Spin System Identification) RC-RNase

1. J-Coupling: $\text{HN} \rightarrow \text{H}_\alpha \rightarrow \text{H}_\beta \dots$ 2. Identify Spin System (a.a. type)



Chapter 10 Two Dimensional Heteronuclear J-correlated Spectroscopy

Advantages of Heteronuclear NMR: There are a number of advantages associated with combining information from heteronuclear spins with that from protons in biomolecular NMR studies, including:

1. The chemical shifts of the heteronuclear spins are more dispersed than proton chemical shifts, thus reducing the overlap of spectral peaks.
2. The relaxation properties of the heteronuclear spin can be easier to interpret than the relaxation of the proton spins, facilitating measurements of protein dynamics.
3. The fixed distance between the proton and the heteronuclear spin facilitates the measurement of bond orientations using residual dipolar couplings, providing an important constraint in structure determination.
4. The one-bond coupling between the amide nitrogen and the carbonyl carbon provides a means to link amino acid spin-systems, facilitating resonance sequential assignments.

Sensitivity of Heteronuclear NMR:

$$\gamma_X^{\frac{5}{2}} / \gamma_H^{\frac{5}{2}}$$

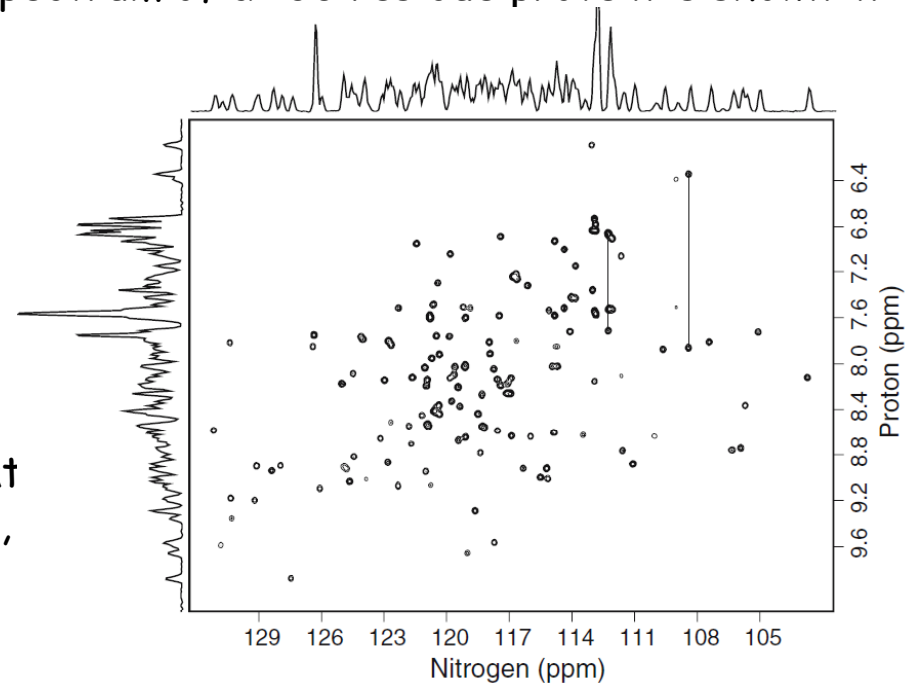
The dependence of the sensitivity on γ is due to two factors. First, a lower γ reduces the population difference between the ground and excited quantum states by a factor that is proportional to γ , as indicated by the Boltzmann distribution. Second, the detection of the precessing magnetization is more sensitive for higher frequency spins, by a factor of $\nu^{3/2}$.

In most applications of heteronuclear NMR, the protein or nucleic acid in the sample is enriched by biosynthetic incorporation of ^{13}C glucose and ^{15}N ammonium to an isotopic enrichment level of 100%. With this level of isotopic enrichment, the sensitivity for ^{13}C is 32 fold less than protons. The situation is worse for ^{15}N , with a 300 fold reduction in sensitivity. Consequently, most heteronuclear NMR experiments are designed to transfer the intense spin polarization of the proton to the heteronuclear spin. The sensitivity of the experiment is increased further by returning the magnetization back to the proton for detection at the end of the experiment.

10.2 Two Dimensional Heteronuclear NMR Experiments

There are three two-dimensional heteronuclear correlation experiments in common use: the heteronuclear multiple quantum coherence (**HMQC**) experiment [10], the heteronuclear single quantum coherence (**HSQC**) experiment [21], and the **refocused- HSQC** experiment. An example of a two-dimensional ^1H - ^{15}N HSQC spectrum of a 130 residue protein is shown in Fig. 10.1.

Figure 10.1. Two-dimensional ^1H - ^{15}N -HSQC spectrum. A two-dimensional HSQC spectrum of a 130 residue protein is represented as a contour plot. The one-dimensional proton and nitrogen spectra are shown on the left side and top of the plot, respectively. Each crosspeak represents a signal from a single N-H pair. The pairs of peaks connected by vertical lines indicate that the two amide protons share the same nitrogen, consequently both peaks have the same nitrogen shift. The HMQC experiment would be almost identical in appearance.

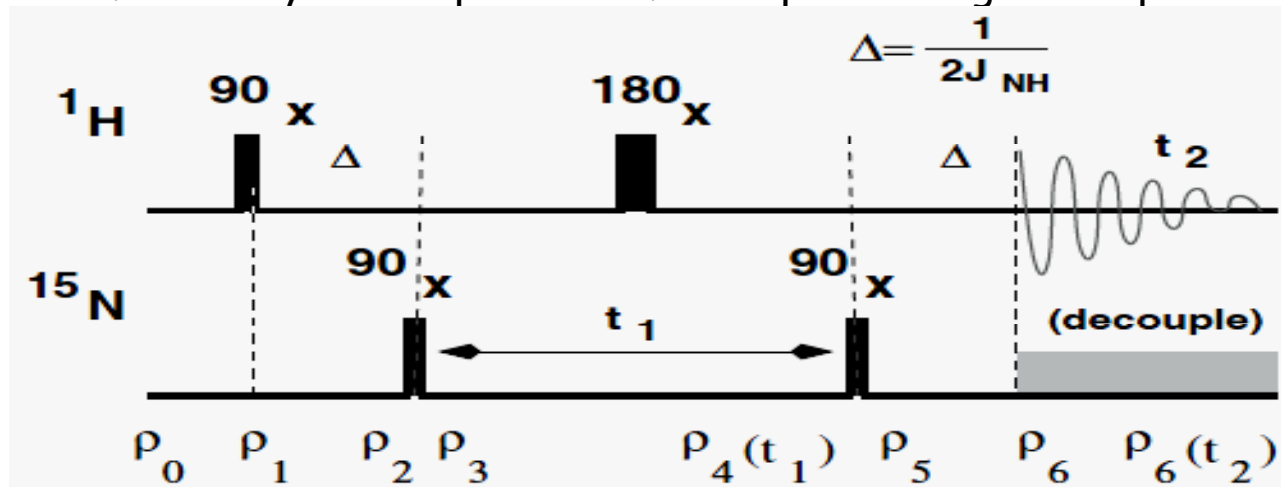


Although these three experiments all generate crosspeaks that correlate the proton and heteronuclear chemical shifts, the experiments differ in the state of the density matrix that evolves during the t_1 (heteronuclear) labeling period. In the case of the HMQC experiment a double-quantum state evolves ($I_x S_x$), the HSQC experiment evolves as an anti-phase single-quantum state ($I_z S_x$), while in the refocused-HSQC experiment the heteronuclear magnetization evolves as pure in-phase magnetization (S_x). Since each of these terms relax at different rates, the linewidths of the resonance peaks in the heteronuclear dimension differ.

In the case of proteins, the refocused HSQC experiment produces the narrowest lines, followed by the HSQC experiment, and lastly the HMQC experiment. Nevertheless, the HMQC experiment can be the most sensitive of the three because it has the fewest number of RF-pulses.

10.2.1 HMQC Experiment

The RF-pulses of proton (Spin I) and heteronuclei (spin S) can be independently altered, thus allows greater flexibility in manipulation of the spins during the experiment.



```

2  d1 do:f2           ;Relaxation Delay(d1), Nitrogen decoupl. off(do:f2)
3  pl2:f2            ;Return N-15 transmitter to high power (level=pl2).
4  (p1 ph0):f1      ;First Pulse, applied to protons on channel 1 (f1)
5  Delta            ;Polarization Transfer Delay
6  (p2 ph0):f2      ;Nitrogen pulse, on channel 2 (f2).
7  d0               ;First Half of Nitrogen evolution time.
8  (p1*2 ph0):f1    ;Refocusing 180 (2 x 90) pulse on protons.
9  d0               ;Second half of Nitrogen evolution time.
10 (p2 ph0):f2      ;Second Nitrogen pulse
11 Delta pl12:f2    ;Second Delta, N-15 power lowered to Pl12 for decoupling.
12 go=2 ph31 cpd2:f2 ;Acquire FID with decoupling applied to Nitrogen
                       ;Loop to label 2 until n scans are acquired.

```

Figure 10.2. HMQC pulse sequence. The upper part of this figure shows the HMQC pulse sequence while the lower part gives a portion of the pulse program code. The pulse program code has been included to illustrate the application of pulses to separate channels and the implementation of decoupling. In the pulse sequence (upper diagram), the upper series of pulses are applied to the proton (*I*) spins while the lower series of pulses are applied to the heteronuclear (*S*) spins, which are ^{15}N in this example. The sequence would be identical for ^{13}C spins, with the appropriate change of the delay Δ . The narrow bars correspond to 90° pulses and the wide bar is a 180° pulse. The time period Δ is nominally set to $\frac{1}{2J}$. Decoupling is applied during acquisition of the proton signal in t_2 . The decoupling scheme is usually WALTZ-16 in the case of ^{15}N or GARP-1 in the case of ^{13}C .

In the pulse program code, *f1* is the proton frequency channel and *f2* is the nitrogen frequency channel. In this example, all pulses are applied along the *x*-axis. In practice they would be phase cycled. The command *pl12:f2*, on line 11, changes the power level (*pl*) of the nitrogen channel from high power to a lower level that is appropriate for decoupling. The command *cpd2:f2*, on line 12, turns on the decoupler during acquisition of the proton FID. After the FID is acquired, the decoupler is turned off at the beginning of the relaxation delay of the next scan (line 2) and the power of the nitrogen channel is reset to high power level for the two nitrogen pulses (line3).

10.2.1.1 Analysis of the HMQC Experiment The HMQC sequence can be divided into five distinct steps:

A	ρ_0	Initial density matrix.
B	$\rho_1 \rightarrow \rho_3$	Transfer of proton polarization to the nitrogen.
C	$\rho_3 \rightarrow \rho_4(t_1)$	Recording the nitrogen chemical shift during t_1 .
D	$\rho_5 \rightarrow \rho_6$	Transfer of nitrogen magnetization back to the proton.
E	$\rho_6 \rightarrow \rho_6(t_2)$	Detection of proton magnetization, amplitude modulated by $e^{i\omega_N t_1}$.

A: Initial Density Matrix.

$$\rho_0 = \gamma_H I_z + \gamma_N S_z$$

A careful analysis of the evolution of the $\gamma_N S_z$ throughout this pulse sequence will show that this term does not generate any detectable magnetization. The gyromagnetic ratio for nitrogen, γ_N , is 1/10 the size of γ_H , thus the contribution from the initial nitrogen magnetization to the final signal is generally minimal, and will be ignored here.

B: Transfer of Proton Polarization to the Nitrogen.

The first 90° pulse on the protons will generate transverse proton magnetization, this will evolve under heteronuclear J-coupling, as follows:

$$\gamma_H I_z \xrightarrow{P_{90}} -\gamma_H I_y \xrightarrow{J} -\gamma_H I_y \cos(\pi J \Delta) + \gamma_H 2I_x S_z \sin(\pi J \Delta) \quad (10.3)$$

$$\text{If } \Delta \text{ is set to } \frac{1}{2J}, \text{ then: } \quad \cos(\pi J \Delta) = 0 \quad \sin(\pi J \Delta) = 1 \quad (10.4)$$

Consequently the cosine term disappears, leaving: $\rho_2 = \gamma_H 2I_x S_z$

This density matrix also evolves due to protein chemical shift because the proton magnetization is transverse, giving:

$$\rho_2 = \gamma_H 2S_z [I_x \cos \omega_I \Delta + I_y \sin \omega_I \Delta]$$

However, this evolution will be canceled by the symmetrically placed, equivalent delay, on the other side of the proton π pulse (see below). Consequently, chemical shift evolution of the protons will be ignored in this interval and only the $\gamma_H 2I_x S_z$ term will be followed.

The second 90° pulse, applied only to the nitrogen spins gives: $\rho_3 = \gamma_H 2I_x S_y$ (10.7)

The presence of the S_y term indicates that the nitrogen has become excited. The intensity of the excited nitrogen state depends on the initial proton polarization, representing transfer of the proton polarization to the nitrogen spin. Note that this product operator represents a multiple (double) quantum transition, hence the name of this experiment.

C: Recording the Nitrogen Chemical Shift.

The density matrix ρ_3 has the potential to evolve during t_1 under the influence of all three terms of the Hamiltonian: J-coupling, proton chemical shift, and nitrogen chemical shift. It will be shown below that there is no evolution of double quantum terms via J-coupling. In addition, the proton chemical shift evolution will be refocused by the proton 180° pulse. Thus, the only *net* change of ρ_3 is due to evolution by the nitrogen chemical shift.

Effect of J-coupling on ρ_3 : The general rule is that density matrices that are represented by the product of two transverse operators, such as, $2I_x S_x$, $2I_y S_y$, $2I_x S_x$, etc. do not evolve due to J coupling, specifically:

$$\begin{aligned} \rho' &= e^{iJ\pi I_z S_z} \rho e^{-iJ\pi I_z S_z} \\ &= \rho \end{aligned}$$

To show that the above holds, consider the example, $\rho = 2I_x S_y$. Evolution of this density matrix under J-coupling for a period arbitrary time τ gives:

$$\begin{aligned}
 2I_x S_y &\xrightarrow{J} 2(I_x \cos\phi + 2I_y S_z \sin\phi)(S_y \cos\phi - 2I_z S_x \sin\phi) \\
 &= 2[I_x S_y \cos^2\phi - 2I_x I_z S_x \cos\phi \sin\phi \\
 &\quad + 2I_y S_z S_y \sin\phi \cos\phi - 4I_y I_z S_z S_x \sin^2\phi] \quad (10.8)
 \end{aligned}$$

($\phi = \pi J\tau$). This expression can be simplified by reducing the three and four product operators (e.g. $I_y I_z S_z S_x$) to pairs of product operators. For example,

$$S_z S_x = \frac{1}{2} \begin{bmatrix} 1 & 0 \\ 0 & -1 \end{bmatrix} \frac{1}{2} \begin{bmatrix} 0 & 1 \\ 1 & 0 \end{bmatrix} = \frac{1}{4} \begin{bmatrix} 0 & 1 \\ -1 & 0 \end{bmatrix} = -i\frac{1}{2} S_y \quad (10.9)$$

The general expression for the above is: $I_\alpha I_\beta = \frac{i}{2} I_\gamma$. Where α, β, γ are cyclic permutations of x, y, z . If the order is reversed, the sign changes, $I_\beta I_\alpha = -\frac{i}{2} I_\gamma$. Using these expressions:

$$\begin{aligned}
 4I_y I_z S_z S_x &= 4\left(\frac{i}{2} I_x\right)\left(\frac{i}{2} S_y\right) = -I_x S_y \\
 2I_x I_z S_x &= 2\left(-\frac{i}{2} I_y\right) S_x = -i I_y S_x \\
 2I_y S_z S_y &= 2I_y \left(-\frac{i}{2} S_x\right) = -i I_y S_x
 \end{aligned}$$

Substituting all of the above into the original equation gives,

Substituting all of the above into the original equation gives,

$$\begin{aligned}
 2I_x S_y &\xrightarrow{J} 2[I_x S_y \cos^2 \phi - 2I_x I_z S_x \cos \phi \sin \phi \\
 &+ 2I_y S_z S_y \sin \phi \cos \phi - 4I_y I_z S_z S_x \sin^2 \phi] \\
 &= 2[I_x S_y \cos^2 \phi + iI_y S_x \cos \phi \sin \phi - iI_y S_x \sin \phi \cos \phi + I_x S_y \sin^2 \phi] \\
 &= 2I_x S_y
 \end{aligned}$$

Therefore, the ρ_3 is unchanged by scalar coupling during t_1 .

Proton Evolution During t_1 - The Spin Echo: The general rule is that a 180° pulse placed in the middle of an interval will result in no *net* evolution of the density matrix via chemical shift. In the case of the HMQC sequence, the 180° pulse in the t_1 evolution time is placed symmetrically; the evolution time before this pulse equals the evolution time after the pulse. Therefore the 180° pulse will refocus any proton chemical shift evolution. This pulse sequence element is called a spin-echo, because the diverging transverse proton magnetization de-phases during the period before the pulse and then re-phases by the end of the time period after the pulse, forming an echo of the original magnetization.

Spin echo sequence: $\tau - 180^\circ - \tau$ causes magnetization to refocus

Skip. Prove this yourselves.

Evolution due to Nitrogen Chemical Shift: The density matrix, $\rho_3 = 2I_xS_y$ evolves with the nitrogen chemical shift as follows:

$$2I_xS_y \xrightarrow{\omega_S t_1} 2I_x[S_y \cos(\omega_S t_1) - S_x \sin(\omega_S t_1)]$$

Therefore the final density matrix after t_1 is simply:

$$\rho_4(t_1) = 2I_xS_y \cos(\omega_S t_1) - 2I_xS_x \sin(\omega_S t_1)$$

Note that the density matrix is now amplitude modulated, carrying information on the nitrogen frequency.

D: Transfer of Magnetization back to the Proton.

The second 90° degree pulse that is applied to the nitrogen produces ρ_5 ,

$$\rho_5 = 2I_xS_z \cos(\omega_S t_1) - 2I_xS_x \sin(\omega_S t_1)$$

The term, $2I_xS_x$ represents double quantum coherence which cannot be detected and will therefore be ignored. The refocusing period, Δ , will transform the single-quantum elements of the density matrix as follows:

$$2I_xS_z \cos(\omega_S t_1) \rightarrow [2I_xS_z \cos(\pi J \Delta) + I_y \sin(\pi J \Delta)] \cos(\omega_S t_1) \quad (10.17)$$

Recall that since $\Delta = \frac{1}{2J}$, the only term that remains at the beginning of signal detection is:

$$\rho_6 = I_y \cos(\omega_S t_1)$$

Again, the proton chemical shift evolution during this period can be ignored. Specifically, the proton chemical shift evolution that occurred during the first Δ period is refocused during the second Δ period because of the 180° proton pulse in the center of the t_1 period.

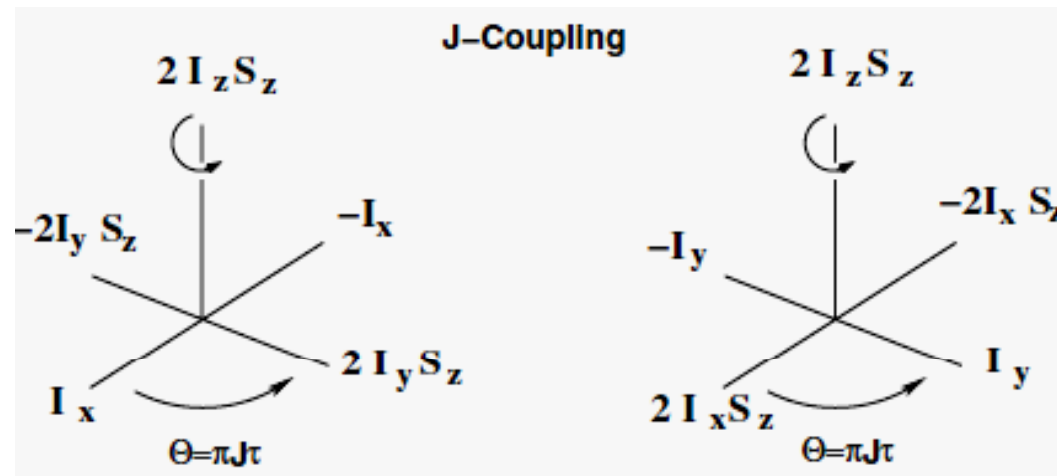
E: Detection.

Decoupling prevents the evolution of the system under J-coupling, thus during the detection period, the density matrix evolves as:

$$\rho_6(t) = \cos(\omega_S t_1) [I_y \cos(\omega_I t_2) - I_x \sin(\omega_I t_2)] \quad (10.19)$$

Giving a detected signal of:

$$S(t_1, t_2) = \gamma_H \cos(\omega_S t_1) e^{i\omega_I t_2} \quad (10.20)$$



It can be shown that product operators containing two transverse terms, such as $2I_x S_y$, do not evolve under J-coupling (see Section 10.2.1.1).

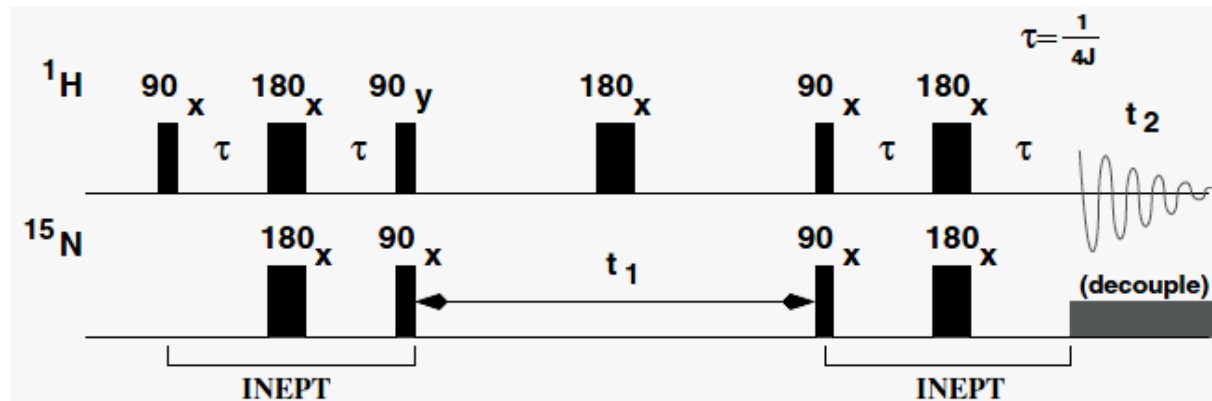
A: Initial Density Matrix.

The initial density matrix is: $\rho_o = \gamma_H I_z + \gamma_N S_z$. For reasons stated in the analysis of the HMQC experiment, the contribution from the heteronuclear spin, $\gamma_N S_z$, can be ignored. Furthermore, the γ_H constant will also be dropped.

10.2.2.1 B: Polarization Transfer - First INEPT.

The first polarization transfer period is referred to as an INEPT¹ transfer and the second polarization period is often referred to as a reverse-INEPT transfer because the magnetization associated with the insensitive spins is transferred back to the attached proton by the same mechanism. For simplicity, the term INEPT will be used to describe this method of magnetization transfer, regardless of the direction of magnetization transfer. The first 90° proton pulse converts I_z (ρ_o) to $-I_y$. Evolution of the proton chemical shift during the remaining part of this period can be ignored because it is a spin-echo sequence ($\tau - 180^\circ - \tau$). Therefore, it is only necessary to consider evolution by J-coupling. The 180° pulses in the middle of the INEPT period are usually applied to both the proton and the heteronuclear spin simultaneously. However, they are considered to occur sequentially in the analysis below. The evolution of the density matrix is as follows ($\phi = \pi J\tau$):

¹INEPT is an acronym for **Insensitive Nuclei Enhanced by Polarization Transfer**



$$\begin{aligned}
 -I_y &\xrightarrow{J} -[I_y \cos(\phi) - 2I_x S_z \sin(\phi)] \\
 &\xrightarrow{180_I^x} -[-I_y \cos(\phi) - 2I_x S_z \sin(\phi)] \xrightarrow{180_S^x} -[-I_y \cos(\phi) + 2I_x S_z \sin(\phi)] \\
 &\xrightarrow{J} \cos(\phi)[I_y \cos(\phi) - 2I_x S_z \sin(\phi)] - \sin(\phi)[2I_x S_z \cos(\phi) + I_y \sin(\phi)] \\
 &= I_y [\cos^2 \phi - \sin^2 \phi] - 2I_x S_z [2\sin(\phi) \cos(\phi)] \\
 &= I_y \cos(2\phi) - 2I_x S_z \sin(2\phi) \tag{10.21}
 \end{aligned}$$

where the trigonometric identities: $\cos(2\phi) = \cos^2 \phi - \sin^2 \phi$ and $\sin(2\phi) = 2\sin \phi \cos \phi$ were used in the last step.

The delay, τ , is set to be equal to $\frac{1}{4J}$, giving $\sin(2\phi) = \sin(2\pi J/[4J]) = \sin(\pi/2) = 1$, therefore the density matrix just before the 90° pulses at the end of the INEPT period is:

$$\rho = -2I_x S_z \tag{10.22}$$

Therefore the INEPT period cause the conversion of in-phase proton magnetization ($-I_y$) to anti-phase magnetization ($2I_x S_z$).

The 90° y -pulse on the proton and x -pulse on the nitrogen convert this to:

$$\rho = -2I_z S_y$$

Note that in contrast to the HMQC sequence, the density matrix in the HSQC experiment is $2I_z S_y$, i.e. the proton magnetization is longitudinal (I_z) and the nitrogen spin is transverse (S_y). Furthermore, note that the total time for polarization transfer is the same in both experiments, $\frac{1}{2J}$.

C: Evolution During t_1 .

During this period the density matrix can potentially evolve under the influence of the proton chemical shift, the heteronuclear chemical shift, and J-coupling.

Evolution of Proton Chemical Shift: Evolution under the proton chemical shift does not occur since the proton state is I_z :

J-Coupling Evolution: Evolution due to J-coupling is refocused by the proton 180° pulse during t_1 . This can be seen with the following analysis ($\zeta = \pi J \frac{t_1}{2}$):

$$\begin{aligned}
 -2I_z S_y &\xrightarrow{t_1/2} -2I_z S_y \cos(\zeta) + S_x \sin(\zeta) \xrightarrow{\pi I_z} +2I_z S_y \cos(\zeta) + S_x \sin(\zeta) \\
 &\xrightarrow{t_1/2} +\cos(\zeta)[2I_z S_y \cos(\zeta) - S_x \sin(\zeta)] + \sin(\zeta)[S_x \cos(\zeta) + 2I_z S_y \sin(\zeta)] \\
 &= -S_x [\cos(\zeta) \sin(\zeta) - \cos(\zeta) \sin(\zeta)] + 2I_z S_y [\cos^2(\zeta) + \sin^2(\zeta)] \\
 &= 2I_z S_y
 \end{aligned}$$

Hence, the only effect of J-coupling on the density matrix during the t_1 period is a change in the sign. This is a general feature of applying a 180° pulse to one of the two coupled spins within a symmetrical interval, there is no net evolution of the density matrix due to J-coupling.

Evolution of Nitrogen Chemical Shift: The net evolution of the density matrix during t_1 is solely due the nitrogen chemical shift:

$$\begin{aligned} 2I_z S_y &\xrightarrow{\omega_S t_1} 2I_z [S_y \cos(\omega_S t_1) - S_x \sin(\omega_S t_1)] \\ &= 2I_z S_y \cos(\omega_S t_1) - 2I_z S_x \sin(\omega_S t_1) \end{aligned} \quad (10.24)$$

D: Polarization transfer back to Protons - The Reverse INEPT.

This segment begins with the pair of x -pulses that are applied to both the proton and heteronuclear spins, interchanging the state of the proton and heteronuclear spins:

$$\begin{aligned} 2I_z S_y \cos(\omega_S t_1) &\rightarrow 2I_y S_z \cos(\omega_S t_1) \\ 2I_z S_x \sin(\omega_S t_1) &\rightarrow -2I_y S_x \sin(\omega_S t_1) \end{aligned} \quad (10.25)$$

Note that the $-2I_y S_x \sin(\omega_S t_1)$ represents double quantum magnetization that cannot be detected during the t_2 period, hence it will be ignored. The subsequent part of the INEPT period ($\tau - 180_{(H,N)}^\circ - \tau$) will refocus the $2I_y S_z$ term to give the density matrix at the beginning of t_2 , i.e.:

$$2I_y S_z \cos(\omega_S t_1) \rightarrow I_x \cos(\omega_S t_1) \quad (10.26)$$

E: Detection.

During the detection period, heteronuclear decoupling is applied so that only a single resonance line is detected for each I-S spin pair, giving the following signal, assuming quadrature detection in t_2 .

$$S(t_1, t_2) = \cos(\omega_S t_1) e^{i\omega_I t_2} \quad (10.27)$$

10.2.3 Refocused-HSQC Experiment

The refocused-HSQC experiment generates pure heteronuclear single quantum coherence, such as S_x or S_y during the t_1 evolution period. The refocused-HSQC experiment is shown in Fig. 10.4. This experiment consists of two back-to-back INEPT transfer periods, a period of nitrogen chemical shift evolution, followed by two additional INEPT periods that return the magnetization to the coupled proton.

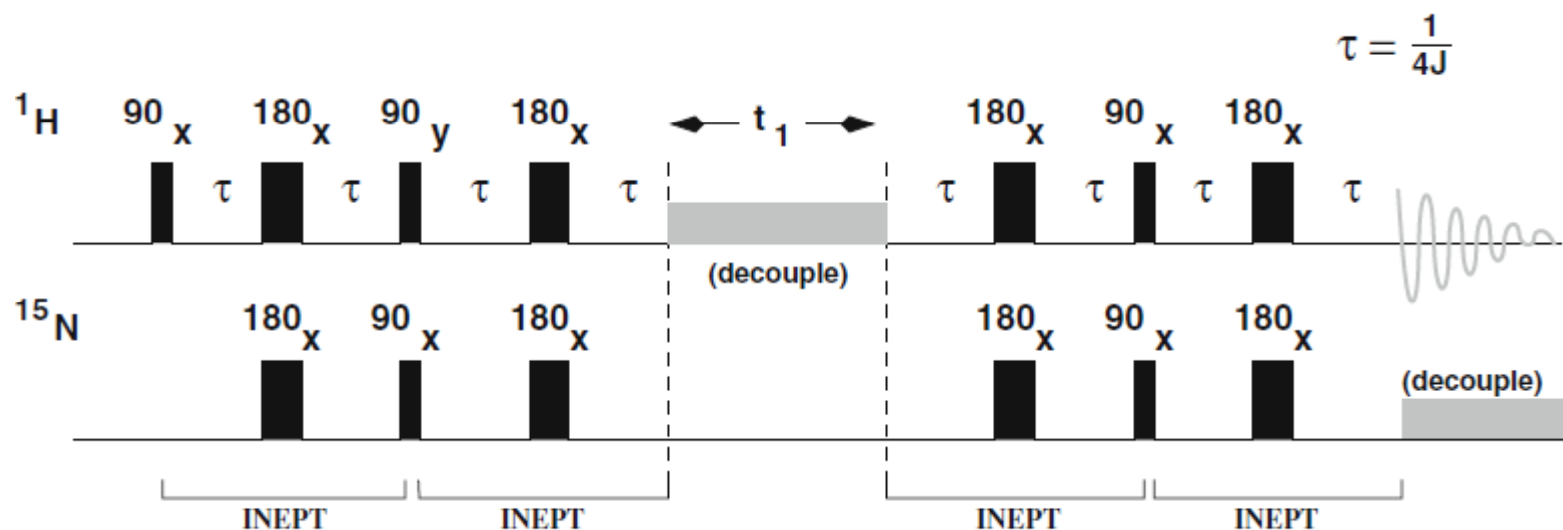


Figure 10.4. Refocused-HSQC experiment. This experiment consists of *two* INEPT blocks, followed by a heteronuclear labeling period, and finishes with two additional INEPT blocks. The two INEPT blocks that bracket the t_1 period serve to inter-convert pure single quantum nitrogen magnetization of the type S_x to proton-nitrogen magnetization of the type $2I_z S_x$. The outer INEPT blocks serve to convert the mixed proton-nitrogen magnetization to pure proton magnetization. Decoupling of the protons is applied during t_1 (DIPSI-2) and decoupling of the heteronuclear spins (WALTZ-16 for ^{15}N and GARP-1 for ^{13}C) is applied during t_2 .

Although the refocused-HSQC experiment appears complex, it can be quickly analyzed by keeping in mind the following rules that describe how the density matrix evolves during an INEPT period:

1. The 180° pulses that are applied to both the proton and the heteronuclear spin will refocus any chemical shift evolution that occurred during the first τ delay.
2. Since 180° pulses are applied to both spins, evolution of the density matrix due to J-coupling will occur during the entire 2τ period. If $\tau = \frac{1}{4J}$ then an in-phase transverse term will evolve to an anti-phase term:

$$I_x \rightarrow 2I_y S_z \quad (10.28)$$

Likewise, an anti-phase term will evolve into in-phase magnetization:

$$2I_y S_z \rightarrow -I_x \quad (10.29)$$

Beginning from the initial density matrix ($\rho_o = I_z$), the evolution of the density matrix to the start of the t_1 period is as follows:

$$I_z \xrightarrow{90_x^I} -I_y \xrightarrow{\tau-180^\circ-\tau} 2I_x S_z \xrightarrow{90_y^I 90_x^S} 2I_z S_y \xrightarrow{\tau-180^\circ-\tau} S_x \quad (10.30)$$

During the t_1 labeling period the density matrix becomes:

$$S_x \xrightarrow{t_1} S_x \cos(\omega_S t_1) + S_y \sin(\omega_S t_1) \quad (10.31)$$

The density matrix does not evolve under J-coupling during this period since the protons have been decoupled. The first INEPT after the t_1 period changes the above density matrix to:

$$S_x \cos(\omega_S t_1) \xrightarrow{\tau-180^\circ-\tau} 2S_y I_z \cos(\omega_S t_1) \xrightarrow{90_x^I 90_x^S} -2S_z I_y \cos(\omega_S t_1) \quad (10.32)$$

$$S_y \sin(\omega_S t_1) \xrightarrow{\tau-180^\circ-\tau} -2S_x I_z \sin(\omega_S t_1) \xrightarrow{90_x^I 90_x^S} 2S_x I_y \sin(\omega_S t_1) \quad (10.33)$$

The second of these terms ($2S_x I_y \sin(\omega_s t_1)$) will not develop into observable magnetization, therefore it will be removed from the analysis. The first term is converted to pure proton magnetization by the last INEPT period:

$$-2S_z I_y \cos(\omega_s t_1) \xrightarrow{\tau - 180^\circ - \tau} I_x \cos(\omega_s t_1)$$

The heteronuclear spin is decoupled during acquisition, so the evolution of the density matrix is solely under the influence of the proton chemical shift. Assuming quadrature detection in t_2 , the final signal is:

$$S(t_1, t_2) = \cos(\omega_s t_1) e^{i\omega_I t_2}$$

10.2.4 Comparison of HMQC, HSQC, and Refocused-HSQC Experiments

The HMQC, HSQC, and refocused-HSQC experiments differ in several attributes, including: the linewidth of resonance lines in the heteronuclear dimension, inherent sensitivity, and the behavior of NH_2 , CH_2 , and CH_3 groups versus NH and CH groups.

10.2.4.1 Comparison of Linewidth

The observed linewidths in the HMQC, HSQC and refocused-HSQC experiments are different due to different relaxation rates and well as to the presence of additional unresolved couplings (see [12] for additional details). The different relaxation rates are due to the presence of different quantum states during t_1 . The magnetization during t_1 is represented by $2I_x S_x$ in the HMQC experiment, as $2I_z S_x$ in the HSQC experiment, and as S_x in the refocused-HSQC experiment. In general, the order of transverse relaxation rates for these terms is: $2I_x S_x > 2I_z S_x > S_x$. In some systems, such as nucleic acids the $2I_z S_x$ term may relax more rapidly, reversing this order. Therefore, the HMQC experiment will have broadest line in the heteronuclear dimension, while the refocused-HSQC will have the narrowest line.

The linewidth of the peaks in the HMQC experiment are broadened further due to proton-proton couplings that are active during the t_1 evolution time. For example, the coupling between the H_N proton and the H_α proton will contribute to the linewidth in ω_1 . Although the 180° pulse in the middle of the t_1 evolution period will refocus both proton evolution and heteronuclear coupling, it cannot refocus homonuclear J-couplings because the 180° pulse effects all protons. Therefore, during t_1 the system evolves as:

$$\rho(t_1) = 2S_y [I_x \cos(\pi J_{HH} t_1) + I_y K_z \sin(\pi J_{HH} t_1)] \quad (10.34)$$

where K_z represents a second proton that is coupled to the proton attached to the heteronuclear spin. This coupling will produce an in-phase splitting of the crosspeaks in the ω_1 frequency domain, thus reducing sensitivity.

In summary, for protein NMR, the HMQC spectrum will have the broadest lines while the refocused-HSQC will produce the narrowest lines.

10.2.5 Sensitivity in 2D-Heteronuclear Experiments

All of these experiments utilize polarization transfer periods to relay the magnetization between the proton and the heteronuclear spin. During these periods, the magnetization also decays due to relaxation. The total transfer time, τ_{total} , in the HMQC and the HSQC experiments are identical, at $1/J$: [$2 \times 1/(2J)$] for the HMQC, [$4 \times 1/(4J)$] for the HSQC experiment. In contrast, the refocused-HSQC experiment requires twice as long, a total of $2/J$. The amount of magnetization that is lost due to relaxation during an HMQC, or INEPT, transfer period is given by the following:

$$e^{-\tau_{total}/\bar{T}_2} \quad (10.35)$$

where, \bar{T}_2 represents the averaged relaxation rate of the magnetization during the transfer period τ_{total} . The loss of intensity due to relaxation is of little significance for a small protein and quite severe for larger proteins. For example, the amide nitrogens in a 10 kDa protein will have an average T_2 of approximately 150 msec, resulting in a signal loss of 7% and 14% for a proton-nitrogen HSQC and a refocused HSQC, respectively. In contrast, the amide nitrogens in a 50 kDa protein have an average T_2 of approximately 20 msec, leading to signal losses of 36% and 77%, respectively, for both experiments, respectively.

Optimal sensitivity in these experiments is obtained when the transfer function in $\sin(\pi Jt)e^{-t/T_2}$ is at a maximum. As shown in Fig. 10.5, the optimal value for the τ delay in the HSQC experiment is always shorter than $\frac{1}{4J}$.

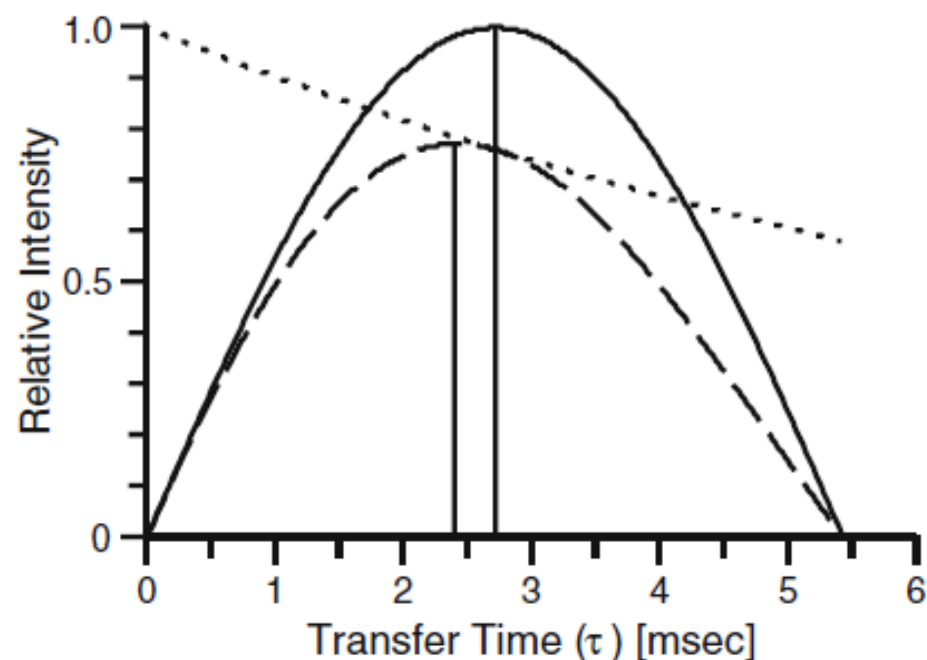


Figure 10.5. Optimization of HSQC delays. The transfer of magnetization during a single INEPT sequence of a ^1H - ^{15}N HSQC experiment as a function of the delay τ is shown. The function plotted is $\sin(\pi J 2\tau) e^{-2\tau/T_2}$. The coupling constant was set to 90 Hz, i.e. $1/(4J) = 2.7$ msec. The overall loss of signal is the square of these curves since two INEPT periods are utilized in this experiment. The solid line shows the transfer function for a small protein while the dashed line shows the transfer function for a ≈ 50 kDa protein. The dotted line shows the decay of magnetization for the 50 kDa protein, assuming a T_2 of 20 msec. The optimal delay, τ , for the large protein is 2.4 msec.

10.2.6 Behavior of XH₂ Systems in HSQC-type Experiments

The above discussion referred to systems in which one proton is attached to one heteronuclear spin (i.e. CH or NH). In many cases two or more protons are attached to heteronuclear spins (e.g. CH₂, CH₃, NH₂). The presence of the additional heteronuclear-proton couplings have to be considered in the analysis of the above sequences.

In the case of both the HMQC and HSQC sequences, the additional proton has no effect on the experiment because the heteronuclear spin is transverse only during the t_1 evolution period. During this time the coupling between the heteronuclear spin and the protons is removed by the 180° refocusing pulse.

In contrast, in the refocused-HSQC experiment the heteronuclear spin is transverse during the *second* INEPT period. During this time it will evolve due to J-coupling with *both* protons. Labeling the protons as I_1 and I_2 and considering evolution due to coupling to the first proton gives:

$$2I_{1z}S_y \xrightarrow{J_1} 2I_{1z}S_y \cos(\pi\tau J_1) + S_x \sin(\pi\tau J_1) \quad (10.36)$$

Further analysis is skipped.

The amount of magnetization transferred by the second INEPT period for CH, CH₂, and CH₃ groups are shown in Fig. 10.6. The dependence of the intensity versus transfer time of NH and NH₂ groups would be the same as the solid and dotted lines, except that the optimal times would be calculated using $J = 90$ Hz.

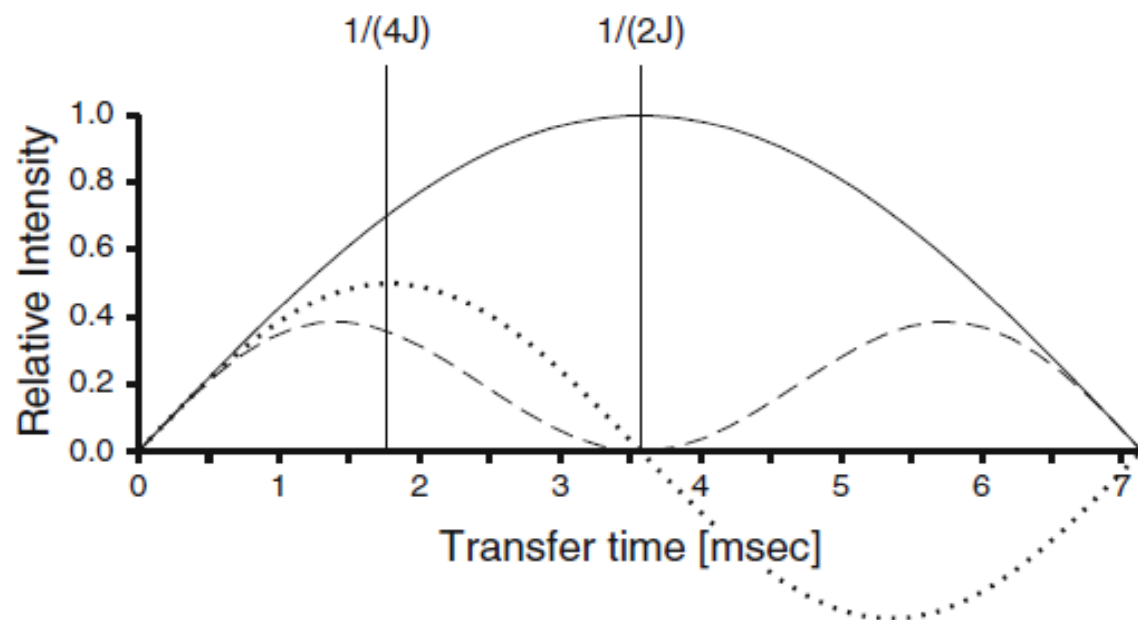


Figure 10.6 Transfer function for a refocused HSQC experiment. Transfer function for CH (solid), CH₂ (dotted) and CH₃ (dashed) groups in a refocused HSQC, assuming a coupling constant of $J = 140$ Hz. The intensity of the magnetization transferred during the second INEPT period of the pulse sequence is shown as a function of total length of the INEPT period (2τ).

This figure shows that a delay of $\tau = 1/(4J)$ is optimal for a CH group while a delay of $\tau = 1/(8J)$ is optimal for a CH₂ group. Furthermore, when the length of the INEPT period is set to $1/(2J)$, the resonance lines from CH₂ and CH₃ groups disappear from the spectra. If the INEPT period is set to longer than $1/(2J)$, the signals from the CH₂ groups will actually become inverted relative to the CH groups.

The dependence of the intensities of signals from the NH₂, CH₂, and CH₃, groups on the length of the INEPT period in refocused-HSQC experiments provides a means to identify such groups. In the case of NH₂ groups on asparagine and glutamine residues, the resonance lines will be absent in a refocused-HSQC experiment if the INEPT delay is set to $1/(2J)$.

